

(19) World Intellectual Property  
Organization  
International Bureau



(43) International Publication Date  
16 September 2004 (16.09.2004)

PCT

(10) International Publication Number  
**WO 2004/079278 A1**

- (51) International Patent Classification<sup>7</sup>: **F24J 2/50**
- (21) International Application Number:  
PCT/CH2004/000130
- (22) International Filing Date: 4 March 2004 (04.03.2004)
- (25) Filing Language: English
- (26) Publication Language: English
- (30) Priority Data:  
PCT/CH03/00156 6 March 2003 (06.03.2003) CH

- (71) Applicant (for all designated States except US): **ECOLE POLYTECHNIQUE FEDERALE DE LAUSANNE (EPFL)** [CH/CH]; CM-Ecublens, CH-1015 Lausanne (CH).
- (72) Inventor; and
- (75) Inventor/Applicant (for US only): **SCHÜLER, Andreas** [DE/CH]; c/o Ecole Polytechnique Fédérale de Lausanne, Ecublens, CH-1015 Lausanne (CH).
- (74) Agent: **ROLAND, André**; Avenue Tissot 15, CH-1001 Lausanne (CH).

(81) Designated States (unless otherwise indicated, for every kind of national protection available): AE, AG, AL, AM, AT, AU, AZ, BA, BB, BG, BR, BW, BY, BZ, CA, CH, CN, CO, CR, CU, CZ, DE, DK, DM, DZ, EC, EE, EG, ES, FI, GB, GD, GE, GH, GM, HR, HU, ID, IL, IN, IS, JP, KE, KG, KP, KR, KZ, LC, LK, LR, LS, LT, LU, LV, MA, MD, MG, MK, MN, MW, MX, MZ, NA, NI, NO, NZ, OM, PG, PH, PL, PT, RO, RU, SC, SD, SE, SG, SK, SL, SY, TJ, TM, TN, TR, TT, TZ, UA, UG, US, UZ, VC, VN, YU, ZA, ZM, ZW.

(84) Designated States (unless otherwise indicated, for every kind of regional protection available): ARIPO (BW, GH, GM, KE, LS, MW, MZ, SD, SL, SZ, TZ, UG, ZM, ZW), Eurasian (AM, AZ, BY, KG, KZ, MD, RU, TJ, TM), European (AT, BE, BG, CH, CY, CZ, DE, DK, EE, ES, FI, FR, GB, GR, HU, IE, IT, LU, MC, NL, PL, PT, RO, SE, SI, SK, TR), OAPI (BF, BJ, CF, CG, CI, CM, GA, GN, GQ, GW, ML, MR, NE, SN, TD, TG).

**Published:**

- with international search report
- before the expiration of the time limit for amending the claims and to be republished in the event of receipt of amendments

For two-letter codes and other abbreviations, refer to the "Guidance Notes on Codes and Abbreviations" appearing at the beginning of each regular issue of the PCT Gazette.

(54) Title: GLAZING

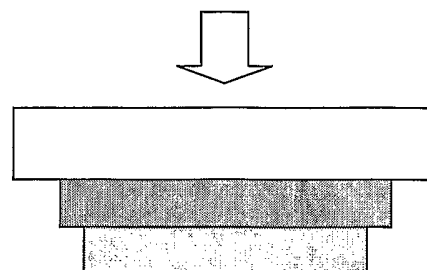
air n = 1

glass n = 1.52

TiO<sub>2</sub> n = 2.2 , varying thickness

SiO<sub>2</sub> n = 1.46 , 140 nm

air n = 1



(57) Abstract: The invention relates to a glazing designed to reflect a narrow spectral band of visible light while being transparent for the rest of the solar spectrum. The glazing is particularly, but not exclusively, suitable for solar collectors.

WO 2004/079278 A1

## GLAZING

### Field of the invention

The present invention relates to glazings which, in particular, may be used in solar collectors.

In the present text, the term "glazing" means any material, e.g. glass or polycarbonate, transparent to visible electromagnetic radiation.

### State of the art

Architectural integration of solar energy systems into buildings is becoming more and more important. Thermal solar collectors, typically equipped with black, optical selective absorbers sheets, exhibit in general good energy conversion efficiencies. However, the black color, and sometimes the visibility of tubes and corrugations of the metal sheets, limits the architectural integration into buildings. Various attempts have been made to overcome this drawback. One way out is to color the absorber sheets. Optical selective absorber coatings are usually deposited by processes such as magnetron sputtering, vacuum evaporation, electrochemical processes, SolGel technology, or as selective paint (thickness-sensitive or thickness-insensitive). These processes are optimised for high solar absorption, yielding typically black or dark blue surfaces. Modifying the process parameters can result in a colored appearance of the solar absorber sheet. Selective paints can be prepared to exhibit blue, green, and brownish red colors. By varying the layer thickness, sputtered absorber coatings can also be colored in a large variety of shades. Following this approach, the absorber surface combines the functions of optical selectivity (high solar absorption/low thermal emission) and colored reflection.

Tripanagnostopoulos et. al. (Y. Tripanagnostopoulos, M. Souliotis, Th. Nousia, Sol. Energy 68, (2000), 343) proposed a different solution, i.e. the use of non-selective colorful paints as absorber coatings for glazed and unglazed collectors, and compensated the energy losses by additional booster reflectors.

### **Summary of the invention**

An object of the present invention is to provide a colored reflection from a glazing, e.g. from the cover glass of a solar collector. This approach has the advantage to separate the functions of optical selectivity and colored reflection, providing thereby more freedom to layer optimization. In addition, if the invention is used in a solar collector, the black, sometimes ugly absorber sheet is hidden by the colored reflection of the glazing.

The principle of the invention is summarised in Figure 1 which schematically shows a thermal solar collector with a colored coating applied to the glazing. The coating reflects a color, thus hiding the corrugated absorber sheet. However the complementary spectrum is transmitted. No absorption occurs in the coating. The coating can be deposited onto the inner of the glazing, as shown in the drawing, but also on the outer side, or on both. Also, a colored coating on the inner side can be combined with a mat outer surface (or with a diffusing substrate). The glazing can consist e.g. of white glass (low iron content), or of organic material such as polycarbonate.

No energy should be lost by absorption in the coating. All non-reflected energy should be transmitted.

Those objectives are achieved with the glazing according to the present invention which, preferably but not exclusively, comprises multilayer interference stacks of transparent materials.

Multilayer interference stacks for various optics and laser applications are known in other fields, see e.g. H. Angus Macleod "Thin-Film Optical Filters", 3<sup>rd</sup> Ed., Institute of Physics Publishing, Bristol, ISBN 0-7503-0688-2 (2001) (2<sup>nd</sup> Ed. with Adam Hilger Ltd, Bristol, ISBN 0-85274-784-5 (1986)).

For the present invention the material choice must be realistic, and the considered refractive indices have consequently to be within a certain range. In addition to that, the maximum number of layers is limited. In contrast to applications such as laser interference filters, solar applications employ typically large surfaces to be coated at low price, which implies that production costs limit the number of individual layers building up the multilayer stack.

One possible way to color the reflected light is the use of thin film interference which is a well known phenomena which can be observed with soap bubbles, thin oil films on water, etc.. The cover glass of a solar collector can be coated, either on one side, or on both. Because of the constraint that no absorption must occur, we preferably use thin films built up of dielectric, transparent materials like e.g.  $\text{SiO}_2$ ,  $\text{Al}_2\text{O}_3$ ,  $\text{TiO}_2$ , composite silicon titanium oxide, or  $\text{MgF}_2$ . Preferably the glass to be coated is practically iron-free ('white' solar glass).

In contrast to photovoltaics, solar thermal collectors can convert the full solar spectrum including the infrared. Thus, in solar collectors, the fraction of invisible but usable solar radiation is much higher than for photovoltaics.

### **List of figures**

Figure 1 schematically illustrates the principle of the invention.

Figure 2 shows the spectrum of the solar radiation and the sensitivity curve of the human eye.

Figure 3 illustrates the ratio "visible reflectance vs. solar loss".

Figure 4 illustrates a first example of the invention.

Figure 5 shows a corresponding reflectance spectra .

Figure 6 shows the color space.

Figure 7 illustrates a second example of the invention.

Figure 8 shows a corresponding reflectance spectra.

Figure 9 shows another reflectance spectra.

Figure 10 illustrates a third example of the invention.

Figure 11 shows a corresponding reflectivity spectra.

Figure 12 shows another reflectance spectra .

Figure 13 illustrates a fourth example of the invention.

Figure 14 shows a corresponding reflectance spectra.

Figure 15 shows another reflectance spectra.

Figure 16 illustrates a fifth example of the invention.

Figure 17 shows a corresponding reflectance spectra.

Figure 18 shows another reflectance spectra.

Figure 19 illustrates a sixth example of the invention.

Figure 20 shows a corresponding reflectance spectra.

Figure 21 shows another reflectance spectra.

Figure 22 shows another reflectance spectra.

Figure 23 shows another reflectance spectra.

Figure 24 shows a reflectivity spectra.

### Detailed description of the invention

For the calculation of the solar absorbance of thermal solar collectors, the solar spectrum at air mass 1.5 (AM1.5) is used conventionally. For the calculation of the solar transmittance  $T_{sol}$  of the colored cover glasses, we also adapt the use of the spectrum AM1.5.

Regarding colorimetry, the Commission Internationale d'Eclairage (CIE) describes standard illuminants (like A, B, C, D65, E). For the determination of the color coordinates of an illuminated surface, we use the standard illuminant D65, that corresponds to a daylight illumination taking into account the diffuse radiation of the sky.

The spectra of D65 and AM1.5 are quite close to each other, but not identical (see Fig. 2).

In order to get an idea of the potential of the envisaged colored glazing with high solar transmission, we calculate the performance of an idealized system that reflects just an extremely narrow spectral band (represented by a  $\delta$ -distribution) and is perfectly transparent for the rest of the solar spectrum. Calculated are the visible reflectance  $R_{VIS}$  under daylight illumination D65, and the solar energy losses by reflection  $R_{sol}$  (%) (based on the solar global spectrum at air mass 1.5). In absence of absorption in films and glass, reflection and transmission are complementary:  $R_{sol}$  (%) +  $T_{sol}$  (%) = 100 %.

By straightforward integration, the ratio  $R_{VIS}$  (%) /  $R_{sol}$  (%) is found to be independent of the amplitude of the narrow spectral band, and depends therefore on the wavelength only (see fig. 3).

In the region from 480 nm to 640 nm, the ratio  $R_{VIS}$  (%) /  $R_{sol}$  (%) is greater than 1. The absolute maximum amounts 6.3 and is reached at 550 nm, which corresponds to a color of yellowish green. This means, that at this wavelength, a visible reflectance of e.g. 12.6 % would just induce solar losses of only 2 %.

Obviously, the ratio  $R_{VIS}$  (%) /  $R_{sol}$  (%) has the character of a figure of merit.

The substrate to be coated is preferably glass. Solar glazing is nearly iron-free, which ensures low absorption in the bulk glass. Typical refractive indices exhibit normal

dispersion in the range of  $1.51 \leq n \leq 1.58$  (at 500 nm:  $n=1.52$  for BK7,  $n = 1.54$  for AF45).

Some commonly used thin film materials are listed below :

| material                | deposition technique   | refractive index n                            |
|-------------------------|--|---|
| $\text{Al}_2\text{O}_3$ | e - beam evaporation,<br>magnetron sputtering,<br>SolGel?    | 1.62 at 600 nm,<br>1.59 at 1600 nm            |
| $\text{MgF}_2$          | evaporation from<br>tantalum boat                            | 1.38 at 550 nm,<br>1.35 at 2000 nm            |
| $\text{SiO}_2$          | e - beam evaporation,<br>magnetron sputtering,<br>SolGel     | 1.46 at 500 nm,<br>1.445 at 1600 nm           |
| $\text{Si}_3\text{N}_4$ | low voltage reactive<br>ion plating,<br>magnetron sputtering | 2.06 at 500 nm                                |
| $\text{TiO}_2$          | e - beam evaporation,<br>magnetron sputtering,<br>SolGel     | 2.2 – 2.7 at 550 nm<br>depending on structure |

Of course there exists many more. Intermediate refractive indices can be achieved by mixing materials to composites (e.g. by mixing  $\text{SiO}_2$  and  $\text{TiO}_2$  to composite silicon titanium oxide). In many cases the refractive indices depend to a large extent on the deposition conditions.

### Numerical simulation of multilayered interference stacks

The optical behavior of multilayered thin film stacks is described by well-known but complicated formulae. Each individual layer is represented by a  $2 \times 2$  matrix, the multilayered stack by their matrix product. Multiple reflections from back and front side of the glass have to be taken into account. Due to the complexity of the equations, numerical simulations are usually performed with the aid of a computer. Software performing these calculations is already commercially available. Spectra-Ray Advanced Fit (SENTECH) is a software originally designed for evaluating ellipsometry data, but it is also capable of straightforward simulation of reflectance and transmittance spectra. A professional tool for designing interference filters is Tfcalc, which also includes the features of refining an existing design and even a global search for optimal designs.

In large area deposition, it is always advantageous to find a solution with the least number of individual layers possible.

#### Example 1 : Refractive Indices 1.46 and 2.2

These refractive indices correspond roughly to  $\text{SiO}_2$  and  $\text{TiO}_2$ , both durable materials accessible by the sol-gel technique as well as by the vacuum techniques of magnetron sputtering or e - beam evaporation. Therefore it is worthwhile to use their combination.

In this example, one side of the glass, which may be the inner side, is coated (see Figure 4).

The effect of varying just a single parameter, the  $\text{TiO}_2$  thickness  $t_{2.2}$ , has been studied.

The graph illustrated in Figure 5 shows the reflectance spectra under variation of the  $\text{TiO}_2$  thickness  $t_{2.2}$  from 0 nm to 80 nm, in steps of 10 nm. The  $\text{SiO}_2$  thickness  $t_{1.46}$  is kept as a constant (140 nm).

The black solid line represents the spectrum for a  $\text{TiO}_2$  thickness  $t_{2.2} = 30$  nm. It shows a sharp maximum at 370 nm, giving rise to a blue-violet color and even a

region of antireflection around 650 nm. Exhibiting acceptable color saturation ( $x = y = 0.22$ ) and a relative luminosity of 8.1 %, the spectrum yields a solar transmission as high as 89.8%.

The locus ( $x, y$ ) in color space can be plotted with the  $\text{TiO}_2$  thickness  $t_{2.2}$  as curve parameter. In Figure 6 the  $\text{TiO}_2$  thickness  $t_{2.2}$  has been running from 0 nm to 1000 nm - point 'A' corresponds to the start at  $t_{2.2} = 0$  nm.

Starting not far from white (point 'D65'), the response of the system is of oscillatory nature. The resulting trajectory is in a certain sense beautiful but illustrates the complexity of the problem: extrema of saturation are of local character (compare points 'B' and 'D').

Color coordinates, visible reflectance and solar transmission for some representative points are given in Table 1.

TABLE 1

| point | $t_{2.2}$ (nm) | x    | y    | approx. color | $R_{\text{vis}}$ (%) | $T_{\text{sol}}$ (%) |
|-------|----------------|------|------|---------------|----------------------|----------------------|
| A     | 0              | 0.3  | 0.32 | white         | 7.5                  | 92.7                 |
| B     | 30             | 0.22 | 0.22 | blue          | 8.1                  | 89.8                 |
| C     | 106            | 0.36 | 0.39 | yellow        | 14.2                 | 86.9                 |
| D     | 152            | 0.2  | 0.19 | blue          | 8.5                  | 88.2                 |
| E     | 300            | 0.22 | 0.37 | green         | 14                   | 88.5                 |
| glass |                | 0.31 | 0.33 |               | 8.2                  | 91.8                 |

( $t_{1.46} = 140$  nm)

A variety of colors can be achieved, keeping the solar transmission above 86 %.

Point 'B' is characterized by excellent solar transmission, only 2 % worse than that of uncoated glass.



Example 2 : Refractive indices 1.38 and 2.2

If a low-index material like  $\text{MgF}_2$  is available ( $n = 1.38$ ), the coloration can be combined with a better partial anti-reflection. Conventionally, this material is deposited by vacuum evaporation. However it is less tough and stable than  $\text{SiO}_2$ .

At one wavelength, the so-called design-wavelength  $\lambda_0$ , the reflection can be made to be zero. Due to the shape of the reflection minimum, this 2-layer design is called "V-coat". This is achieved by choosing the appropriate film thicknesses  $t_{1.38}$  and  $t_{2.2}$ .

Coating both sides of the glass enhances color saturation and the effect of anti-reflection (see Figure 7).

Figure 8 visualizes the reflectance spectra for design-wavelengths  $\lambda_0 = 650 \text{ nm}$  and  $1300 \text{ nm}$ .

By scaling the film thickness, interference minima and maxima can be shifted easily in wavelength, thus giving rise to a variety of colors (see TABLE 2).

TABLE 2

| $\lambda_0$ | $t_{2.2} \text{ (nm)}$ | $t_{1.38} \text{ (nm)}$ | x     | y     | approx. color | $R_{\text{vis}} \text{ (%)}$ | $T_{\text{sol}} \text{ (%)}$ |
|-------------|------------------------|-------------------------|-------|-------|---------------|------------------------------|------------------------------|
| 600         | 16                     | 140                     | 0.15  | 0.1   | violet        | 1.44                         | 94                           |
| 650         | 17                     | 151                     | 0.16  | 0.15  | blue          | 3.64                         | 93.4                         |
| 700         | 19                     | 163                     | 0.19  | 0.2   | blue          | 7.7                          | 92.2                         |
| 800         | 21                     | 186                     | 0.23  | 0.27  | blue-green    | 16                           | 90.7                         |
| 900         | 24                     | 209                     | 0.28  | 0.34  | green         | 23.4                         | 88.9                         |
| 1000        | 27                     | 233                     | 0.35  | 0.41  | yellow-green  | 26.1                         | 87.5                         |
| 1200        | 32                     | 279                     | 0.39  | 0.32  | white         | 16.8                         | 82.2                         |
| 1300        | 35                     | 302                     | 0.3   | 0.2   | purple        | 11.5                         | 83.9                         |
| 1400        | 37                     | 326                     | 0.22  | 0.18  | violet        | 11.4                         | 82.9                         |
|             | glass                  |                         | 0.313 | 0.329 |               | 8.17                         | 91.8                         |

The solar transmission  $T_{\text{sol}}$  can even be made higher than the one of uncoated glass, nevertheless keeping considerable luminosities in the violet and blue, up to nearly 8%! In the yellow-green, a luminosity of 26.1 % is achieved, the losses are only 4.4 % worse compared to the uncoated glass!

### Example 3 : V-coat or W-coat

For two-layered systems, the nicknames "V-coat" and "W-coat" indicate special anti-reflection designs. The names are derived from the form of the spectra: a V-coat has one minimum, a W-coat two ones. For the latter one, the region of low reflection is broader.

model: air//LH//glass//HL//air

With "design-wavelength"  $\lambda_0$  :  $n \times t(\text{H}) = \lambda_0/2$     $n \times t(\text{L}) = \lambda_0/4$

$n(\text{H}) = 1.8, 2.2$

$n(\text{L}) = 1.38, 1.47$

Figure 9 shows the reflection spectra for a design-wavelength of 800 nm.

For the shown examples, the resulting colors are in the region of bluish green. Due to the partial antireflection, the achieved color saturation and as well the solar transmission are remarkable (see Table 3).

TABLE 3

| $n(\text{H})$ | $n(\text{L})$ | $t(\text{H})$ | $t(\text{L})$ | x    | y    | $R_{\text{VIS}} (\%)$ | $T_{\text{sol}} (\%)$ |
|---------------|---------------|---------------|---------------|------|------|-----------------------|-----------------------|
| 1.8           | 1.47          | 222           | 136           | 0.18 | 0.27 | 9.1                   | 92.5                  |
| 2.2           | 1.47          | 182           | 136           | 0.21 | 0.32 | 21.1                  | 86.2                  |
| 1.8           | 1.38          | 222           | 145           | 0.19 | 0.29 | 9.4                   | 93.4                  |
| 2.2           | 1.38          | 182           | 145           | 0.23 | 0.34 | 23.3                  | 85.7                  |

Example 4 : Three-layered system

Adding an additional layer to a V-design results in a strong enhancement of the colored reflection (see Figure 10).

The reflectivity is computed for normal incidence (see Figure 11).

The spectrum corresponding to the case of a 30 nm thick top layer exhibits a strong enhancement of the reflection peak and still a region of partial anti-reflection at a wavelength of 1000 nm. For the top layer being 50 nm thick, the region of anti-reflection is already less pronounced.

The table 4 shows the numerical results in dependence on the thickness  $t_3$  of the third layer (the topmost one).

TABLE 4

| $t_3$ (nm) | x    | y    | $R_{VIS}$ (%) | $R_{sol}$ (%) | $T_{sol}$ (%) |
|------------|------|------|---------------|---------------|---------------|
| 0          | 0.22 | 0.22 | 8.1           | 10            | 90            |
| 10         | 0.24 | 0.27 | 17            | 12            | 88            |
| 20         | 0.27 | 0.31 | 28            | 16            | 84            |
| 30         | 0.29 | 0.34 | 37            | 20            | 80            |
| 40         | 0.31 | 0.36 | 43            | 24            | 76            |
| 50         | 0.34 | 0.38 | 46            | 27            | 73            |

Also from the point of view of the solar transmission  $T_{sol}$ (%), the region between 10 nm and 40 nm appears most interesting.

Towards shorter wavelengths, the reflectance spectra for dielectric thin film stacks exhibit rapid oscillations between the maxima and minima of higher order. By using high enough thickness of the individual layers, these maxima can be chosen to be located in the visible spectral region.

Here, the computation of color coordinates is based on the CIE illuminant C. Fortunately, the materials SiO<sub>2</sub> and TiO<sub>2</sub> are included, assuming the refractive indices listed in table 5.

TABLE 5

| wavelength<br>(nm) | TiO <sub>2</sub> | SiO <sub>2</sub> |
|--------------------|------------------|------------------|
| 300                | 2.6              | 1.48             |
| 400                | 2.52             | 1.47             |
| 500                | 2.42             | 1.46             |
| 600                | 2.35             | 1.45             |
| 700                | 2.33             | 1.45             |
| 800                | 2.3              | 1.44             |

Figure 12 illustrates an example showing the rapid oscillations in the high wavelength region and the peaks in the visible which are used for the coloration: for a color of pink, two peaks in the blue and in the red, are necessary.

In this case, color coordinates of  $x = 0.39$  ,  $y = 0.24$  are found, with a visible reflectance of 9.8 % - the solar transmission amounts 84.6 %. Layer thickness of 213 nm and 258 nm are assumed for the TiO<sub>2</sub> and the SiO<sub>2</sub> layers, respectively. Only one side of the glass is assumed to be coated.

Some more examples are listed in Table 6. The selection comprises two, three and four layered systems.

TABLE 6

| design | layer                         |                               |                               |                               | color coordinates |      | approx.<br>Color | R <sub>vis</sub><br>(%) | T <sub>sol</sub> (%) |
|--------|-------------------------------|-------------------------------|-------------------------------|-------------------------------|-------------------|------|------------------|-------------------------|----------------------|
|        | 1<br>TiO <sub>2</sub><br>(nm) | 2<br>SiO <sub>2</sub><br>(nm) | 3<br>TiO <sub>2</sub><br>(nm) | 4<br>SiO <sub>2</sub><br>(nm) | x                 | y    |                  |                         |                      |
| A      | 213                           | 258                           |                               |                               | 0.39              | 0.24 | pink             | 9.8                     | 84.6                 |
| B      | 126                           | 304.34                        |                               |                               | 0.22              | 0.14 | blue             | 6.7                     | 83.6                 |
| C      | 15                            | 410                           |                               |                               | 0.35              | 0.42 | yellow           | 13.9                    | 90.4                 |
| D      | 88                            | 224                           |                               |                               | 0.48              | 0.38 | orange           | 16.1                    | 82.7                 |
| E      | 11.5                          | 378                           | 11.5                          |                               | 0.35              | 0.41 | yellow           | 16.9                    | 88.5                 |
| F      | 21                            | 45                            | 259                           | 109                           | 0.22              | 0.15 | blue             | 6.3                     | 88.4                 |
| G      | 11.5                          | 378                           | 11.5                          | 378                           | 0.29              | 0.39 | green            | 14                      | 89.7                 |
| H      | 104                           | 37                            | 103                           | 231                           | 0.52              | 0.35 | orange           | 15.5                    | 80.3                 |

Layer 1 is the next to the glass. Refractive index for the glass :  $n = 1.52$  , coating only on one side.

Often, quarter wave interference stacks are designed as broadband reflection filters, consisting of numerous individual layers and exhibiting a nearly perfect reflection over a broad frequency range. In contrast to this, we focus on filters reflecting just a narrow frequency band, and we will show how it is possible to achieve reasonable results with only a few of individual layers.

#### Example 5 : Narrow peak by many $\lambda/4$ layers

Stacks of  $\lambda/4$  layers are frequently used to generate high reflectivity mirrors exhibiting a broad band of reflection.

However, by choosing the refractive indices of the two involved materials close to each other, narrow reflection peaks can be produced. If the refractive indices are really close, a lot of layers are however needed to produce a reasonable amplitude.

The present example refers to a system consisting of 40 individual layers. As shown further in the text, such a great number of layers is not preferred for the present invention and should therefore be considered like a comparative example.

We consider (see Figure 13) the reflection of just one coated surface, which corresponds to the situation where the other surface of the glazing is perfectly "anti-reflected".

The resulting reflectance (see Figure 14) spectrum exhibits a sharp peak at  $\lambda = 550$  nm.

The FWHM amounts 21 nm, the spectrum yielding

$$x=0.31 \quad y = 0.47 \quad R_{VIS} = 9.1 \%$$

If one assumes that the other side of substrate is neither anti-reflected nor coated, the resulting color is a little less saturated:

$$x=0.31 \quad y = 0.41 \quad R_{VIS} = 12.7 \%$$

The peak position can be chosen freely and is controlled by the scale of the optical thicknesses of the individual layers :  $n \times t = \lambda/4$

The position of the peak depends on the angle of reflection, therefore also the color is angular-dependent (see Figure 15).

For angles of  $0^\circ$ ,  $20^\circ$ ,  $40^\circ$  and  $60^\circ$  one gets a different position of the maximum, 550 nm, 535 nm, 496 nm and 447 nm, respectively. The background level rises for high angles, leading to less saturated colors.

#### Example 6 : System with a few layers

For a large area application, it is advisable to reduce the number of individual layers. In order to achieve a reasonable peak height, the refractive indices must exceed a minimum of difference (see Figure 16). However, if they are too different, the peak is too broad.

Refractive indices correspond to  $\text{SiO}_2$  (L) and  $\text{Al}_2\text{O}_3$  (H).

To achieve a nice peak with this choice of refractive indices, it is important that the first and the last layers consist of the high index material (phase shifts).

Let us consider the evolution of the reflectance peak, while successive layers are added (increasing m).

Figure 17 shows the calculated reflectance spectra for 3 to 15 layers (m from 1 to 7).

Increasing the number of layers leads to increasing color saturation and visible reflectance. Values for color coordinates x, y,  $R_{\text{VIS}}$  (%), and height and width of reflection peak  $R_{\text{max}}$ , FWHM (full width at half maximum) are given in TABLE 7.

TABLE 7

| m | x    | y    | R <sub>vis</sub> (%) | R <sub>max</sub> | FWHM (nm) |
|---|------|------|----------------------|------------------|-----------|
| 7 | 0.33 | 0.56 | 40.4                 | 0.64             | 76        |
| 6 | 0.33 | 0.55 | 37.7                 | 0.57             | 81        |
| 5 | 0.34 | 0.54 | 34.5                 | 0.49             | 90        |
| 4 | 0.35 | 0.53 | 30.6                 | 0.41             | 102       |
| 3 | 0.36 | 0.5  | 25.9                 | 0.32             | 124       |
| 2 | 0.35 | 0.45 | 20.4                 | 0.23             | 156       |
| 1 | 0.33 | 0.38 | 14.2                 | 0.15             | 234       |

For five layers ( $m = 2$ ), the values seem already to be reasonable.

Figure 18 shows the case of a 5 layer object where the refractive index of material H is changed, keeping its optical thickness  $n(H) \times t(H)$  always to  $\lambda/4$  ( $\lambda = 550$  nm).

The spectrum for  $n(H) = 1.65$  has already been known from the last calculation and is again represented by the black solid line.

By changing the difference of the refractive indices  $n(H) - n(L)$ , the peak height can be easily controlled. Considerable peak heights can be achieved without too excessive peak broadening (see Table 8).

TABLE 8

| n(H) | t(H) (nm) | x    | y    | R <sub>vis</sub> (%) | R <sub>max</sub> | FWHM (nm) |
|------|-----------|------|------|----------------------|------------------|-----------|
| 1.55 | 89        | 0.34 | 0.42 | 9.4                  | 0.1              | 144       |
| 1.6  | 86        | 0.35 | 0.44 | 14.6                 | 0.16             | 152       |
| 1.65 | 83        | 0.35 | 0.45 | 20.4                 | 0.23             | 156       |
| 1.7  | 81        | 0.36 | 0.46 | 26.5                 | 0.3              | 164       |
| 1.75 | 79        | 0.36 | 0.46 | 32.7                 | 0.36             | 174       |
| 1.8  | 76        | 0.35 | 0.45 | 38.7                 | 0.43             | 180       |

( $n(L) = 1.47$ ,  $t(L) = 93$  nm.)

Example 6 : Full system

The full system includes the two surfaces of the glass: one or both could be coated.

one side coated:            air//glass//HLHLH //air

combination with AR:    air//AR//glass//HLHLH //air

In a SolGel dip - coating process, both sides of the glass can be coated symmetrically at the same time (see Figure 19) as follows :

air//HLHLH//glass//HLHLH //air

As expected, coating both sides of the substrate identically leads to much higher peaks (see Figure 20).

The black solid line represents again the system with  $n(H) = 1.65$ .

The peaks get slightly broader, but not much. For  $n(H) = 1.65$  this means a FWHM of 167 nm instead of 156 nm. However, this does not harm the color saturation considerably (see Table 9).

TABLE 9

| n(H) | t(H) (nm) | R <sub>max</sub> | FWHM (nm) | x    | y    | R <sub>vis</sub> (%) | T <sub>sol</sub> (%) |
|------|-----------|------------------|-----------|------|------|----------------------|----------------------|
| 1.55 | 89        | 0.19             | 152       | 0.34 | 0.41 | 17.2                 | 89.7                 |
| 1.65 | 83        | 0.37             | 167       | 0.35 | 0.44 | 33.7                 | 84.2                 |
| 1.75 | 79        | 0.53             | 186       | 0.36 | 0.44 | 49                   | 78.3                 |

For  $n(H) = 1.55$ , the glass has only lost 2.1 % of solar transmission relative to an uncoated glass ( $T_{sol} = 91.7\%$ ), yielding a visible reflectance of 17.2 %. Even higher visible reflectance of 33.7 % is found for  $n(H) = 1.65$ , the losses relative to the uncoated glass amount just 7.6 %.



The peak position and thus the color can be controlled by scaling the optical film thicknesses to a quarter of the design wavelength  $\lambda_0$ .

With  $n(H) = 1.65$ ,  $n(L) = 1.47$  we obtain the representative spectra depicted at Figure 21.

The chosen peak positions correspond to colors of blue, green and orange, respectively (see Table 10).

TABLE 10

| $\lambda_0$ | t(H) (nm) | t(L) (nm) | x    | y    | approx. Color | R <sub>vis</sub> (%) | T <sub>sol</sub> (%) |
|-------------|-----------|-----------|------|------|---------------|----------------------|----------------------|
| 450         | 68        | 77        | 0.2  | 0.24 | blue          | 17.1                 | 86.1                 |
| 550         | 83        | 93        | 0.35 | 0.44 | green         | 33.7                 | 84.2                 |
| 650         | 98        | 111       | 0.44 | 0.36 | orange        | 20                   | 83.8                 |

Figure 22 shows the angular dependence of the spectra for the system with  $n(H) = 1.65$ ,  $n(L) = 1.47$ ,  $\lambda_0 = 550$  nm.

The quantification is presented in the Table 11.

TABLE 11

| angle | pos. of max. (nm) | x    | y    | R <sub>vis</sub> (%) | T <sub>sol</sub> (%) | T <sub>glass</sub> (%) | loss rel. to glass (%) |
|-------|-------------------|------|------|----------------------|----------------------|------------------------|------------------------|
| 0°    | 548               | 0.35 | 0.44 | 33.7                 | 84.2                 | 91.8                   | 7.6                    |
| 20°   | 534               | 0.32 | 0.42 | 33                   | 84.4                 | 91.8                   | 7.4                    |
| 40°   | 499               | 0.27 | 0.35 | 28.5                 | 84.2                 | 91                     | 6.8                    |
| 60°   | 456               | 0.25 | 0.29 | 24                   | 79.8                 | 84.4                   | 4.6                    |
| 80°   |                   | 0.3  | 0.33 | 55.6                 | 44.6                 | 45.7                   | 1.1                    |

For raising angles, one notes a blue shift of the maximum. The losses relative to the uncoated glass (solar transmission T<sub>glass</sub>) tend to decrease, the color saturation, however, too (increasing level of background).

Now, we would like to lower the level of background oscillation. Therefore we choose both indices of refraction  $n(H)$  and  $n(L)$  to be lower than the one of glass.

model: air//(HL)<sup>3</sup>//glass//(HL)<sup>3</sup>//air

L: MgF<sub>2</sub>      n(L) = 1.38

H: SiO<sub>2</sub>      n(H) = 1.47

To take into account the phase jump relations, the coating is of the form (HL)<sup>m</sup>.

The resulting spectra is illustrated on Figure23.

For normal incidence, the level of oscillation could indeed be lowered to a value of 6% instead of 9 %, thus gaining some percent in solar transmission.

The quantification is shown on Table 12.

TABLE 12

| angle | pos. of<br>max. (nm) | x    | y    | R <sub>vis</sub> (%) | T <sub>sol</sub> (%) | T <sub>glass</sub> (%) | loss rel. to<br>glass (%) |
|-------|----------------------|------|------|----------------------|----------------------|------------------------|---------------------------|
| 0°    | 549                  | 0.36 | 0.48 | 20.8                 | 90.6                 | 91.8                   | 1.2                       |
| 20°   | 534                  | 0.32 | 0.47 | 20                   | 90.7                 | 91.8                   | 1.1                       |
| 40°   | 490                  | 0.22 | 0.33 | 14.6                 | 90.2                 | 91                     | 0.8                       |
| 60°   | 436                  | 0.25 | 0.23 | 13.1                 | 84.7                 | 84.4                   | -0.3                      |
| 80°   | 397                  | 0.31 | 0.32 | 52.5                 | 46.5                 | 45.7                   | -0.8                      |

In this example, the transmission losses relative to the uncoated glass are really small or even negative (which means gains) – in spite of considerable relative luminance.

The numerical simulation can also be used to monitor the different preparation stages of a multilayered coating. If samples are produced with e.g. 1, 2, 3, 4 & 5 individual layers, the measured spectra can be compared to the theoretical targets. Refractive indices are taken here as measured by experimental methods such as ellipsometry and *in situ* laser reflectometry.

model :

| # of layer | material                       | ref. index | thickness (nm) |
|------------|--------------------------------|------------|----------------|
| 0          | glass                          | 1.52       |                |
| 1          | Al <sub>2</sub> O <sub>3</sub> | 1.6        | 93             |
| 2          | SiO <sub>2</sub>               | 1.48       | 86             |
| 3          | Al <sub>2</sub> O <sub>3</sub> | 1.6        | 93             |
| 4          | SiO <sub>2</sub>               | 1.48       | 86             |
| 5          | Al <sub>2</sub> O <sub>3</sub> | 1.6        | 93             |

Figure 24 shows the theoretical normal reflection as the successive layers are added .

At the design wavelength (here 550 nm), adding the individual layers successively results in alternating enhanced reflection or anti-reflection.

Other experimental results are listed below :

**sample I :**

glass substrate // 30 nm TiO<sub>2</sub> // 140 nm SiO<sub>2</sub>

**sample II :**

glass substrate // 30 nm TiO<sub>2</sub> // 140 nm SiO<sub>2</sub> // 30 nm TiO<sub>2</sub>

**sample III :**

glass substrate // 30 nm TiO<sub>2</sub> // 140 nm SiO<sub>2</sub> // 30 nm TiO<sub>2</sub> // 140 nm SiO<sub>2</sub> // 30 nm TiO<sub>2</sub>

**sample IV :**

glass substrate // 45 nm TiO<sub>2</sub> // 210 nm SiO<sub>2</sub>

**sample V :**

glass substrate // 45 nm TiO<sub>2</sub> // 210 nm SiO<sub>2</sub> // 45 nm TiO<sub>2</sub>

**sample VI :**

glass substrate // 45 nm TiO<sub>2</sub> // 210 nm SiO<sub>2</sub> // 45 nm TiO<sub>2</sub> // 210 nm SiO<sub>2</sub> // 45 nm TiO<sub>2</sub>

TABLE 13

| sample | color x | color y | R(vis)[%] | T(sol)[%] | loss[%] | M=R(vis)/loss |
|--------|---------|---------|-----------|-----------|---------|---------------|
| I      | 0.26    | 0.25    | 9         | 92        | 8       | 1.13          |
| II     | 0.24    | 0.26    | 16        | 89        | 11      | 1.45          |
| III    | 0.2     | 0.22    | 18        | 87        | 13      | 1.38          |
| IV     | 0.28    | 0.33    | 20        | 90        | 10      | 2.00          |
| V      | 0.38    | 0.41    | 26        | 85        | 15      | 1.73          |
| VI     | 0.32    | 0.29    | 15        | 82        | 18      | 0.83          |

The table shows the CIE color coordinates x, y, the visible reflectance  $R_{VIS}$  under daylight illumination D65, the solar transmission  $T_{sol}$  for a solar spectrum AM1.5 global, the solar energy loss, and the figure of merit  $M = R_{VIS} / \text{loss}$ , as determined for the samples I to VI by spectrophotometry.

The colored thin film interference stack can also be located between two "thick" layers (e.g. a substrate and "thick" transparent top layer). "Thick" means here a thickness larger than the coherence length of the light. This will reduce the color change induced by water droplets condensing eventually on the inner side of the collector glazing or being formed on the outer side, respectively.

The following procedure illustrates a general approach which can be used in order to define the most appropriate glazing for a specific use :

- i. rough concept of coating design by theoretical calculation with assumed values for the index of refraction
- ii. literature data of material properties  $\Rightarrow$  choice of materials
- iii. deposition of individual layers of chosen materials
- iv. experimental determination of optical properties (n, k) and film thicknesses (t) of real samples (individual layers): spectroscopic ellipsometry, spectrophotometry
- v. optimization of coating design for the real material properties taking into account the dispersion of refractive index - recommended software Tfcalc

- vi. finding process parameters for the right film thicknesses (magnetron sputtering: e.g. deposition time, input power // SolGel dip - coating: e.g. withdrawing speed, viscosity)

loop: coating deposition

↓            ↑

optical measurement of thickness

- vii. deposition of multilayered coating
- viii. measurement of reflection and transmission spectra of multilayered coating, comparison with predictions of theory
- ix. in case of deviations: adaptation of the process

Other References

1. Alfred Thelen "Design of Optical Interference Coatings", McGraw-Hill, New York, ISBN 0-0-063786-5 (1989)
2. Alfred Thelen "Design of Multilayer Interference Filters", in "Physics of Thin Films", ed. by Georg Hass and Rudolf E. Thun, Academic Press, New York, Vol. 5, p. 47 (1969)
3. Oliver S. Heavens "Optical Properties of Thin Solid Films", Butterworths, London (1955)
4. Kurt Nassau, "The Physics and Chemistry of Color – The Fifteen Causes of Color", John Wiley & Sons, New York, ISBN 0-471-86776-4 (1983)
5. Robert Sève, "Physique de la couleur – de l'apparence colorée à la technique colorimétrique", Masson, Paris, ISBN 2-225-85119-0 (1996)
6. International Commission on Illumination CIE, Colorimetry, CIE Publication 15.2., 2<sup>nd</sup> Ed., ISBN 3-900-734-00-3, Vienna, (1986)

## Claims

1. Glazing characterized by the fact that it comprises selective reflecting means adapted to exclusively reflect a narrow spectral band of visible light while being transparent for the rest of the solar spectrum.
2. Glazing according to claim 1 wherein said selective reflective means comprise an interference filter.
3. Glazing according to any of the previous claims wherein said selective reflective means comprise multi-layer interference stacks.
4. Glazing according to any the previous claim wherein said selective reflective means are located between two layers having each a thickness larger than the coherence length of the light.
5. Glazing according to any of the previous claims wherein said selective reflective means are located at the inner side of the glazing.
6. Glazing according to any of the previous claims 1 to 5 wherein said selective reflective means are located at the outer side of the glazing.
7. Glazing according to any of the previous claims comprising a light-diffusing layer, or a light-diffusing rough surface, or a light-diffusing rough interface
8. Glazing according to any of the previous claims designed in a such a way that said narrow spectral band corresponds to a ratio "visible reflectance  $R_{vis}$  / solar energy loss  $R_{sol}$ " which is higher than 1.2.
9. Solar collector comprising a glazing according to any of the previous claims.

FIG. 1

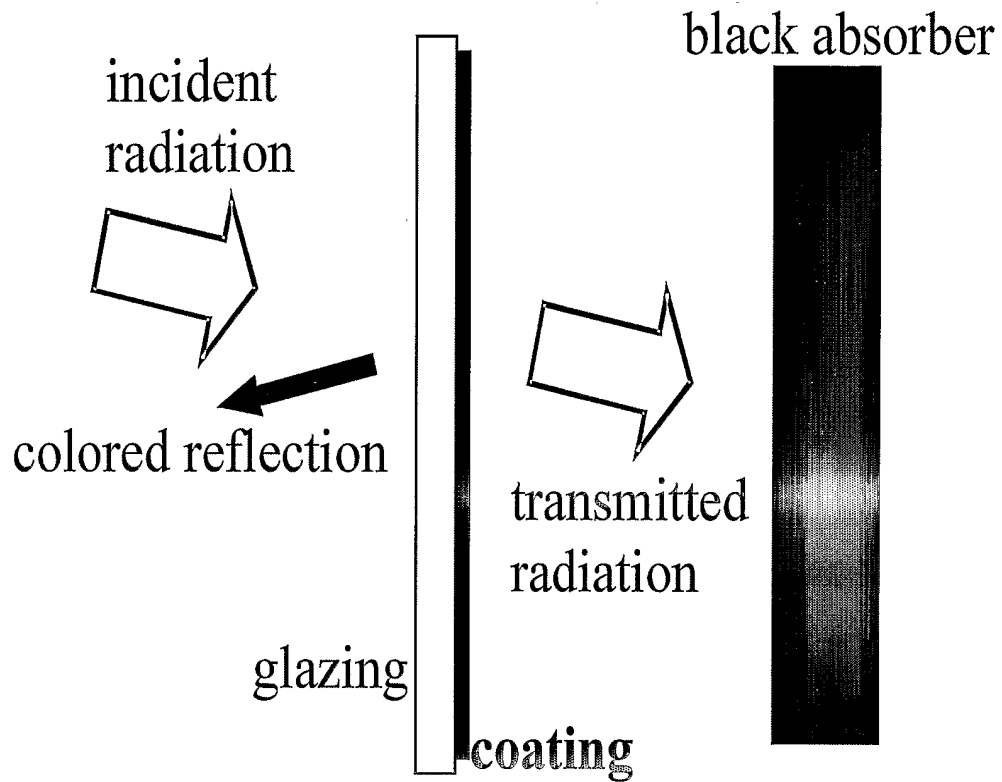
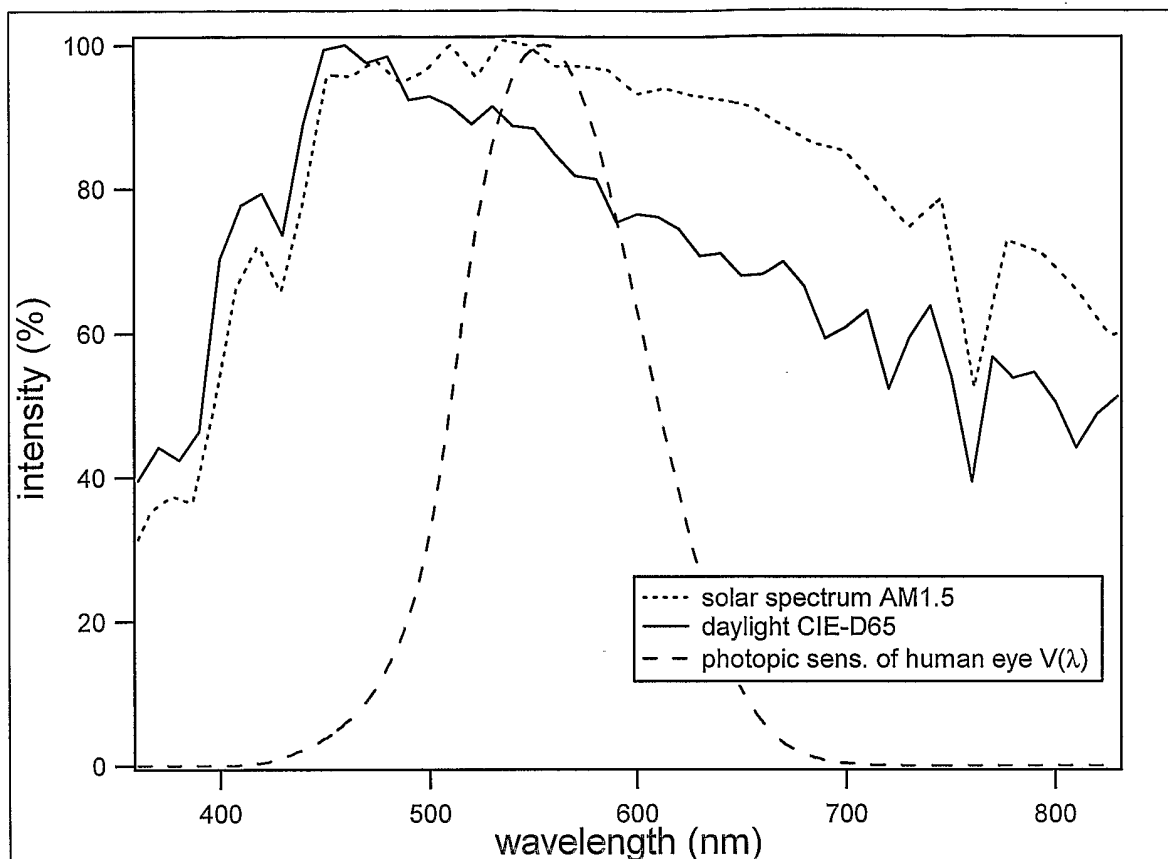
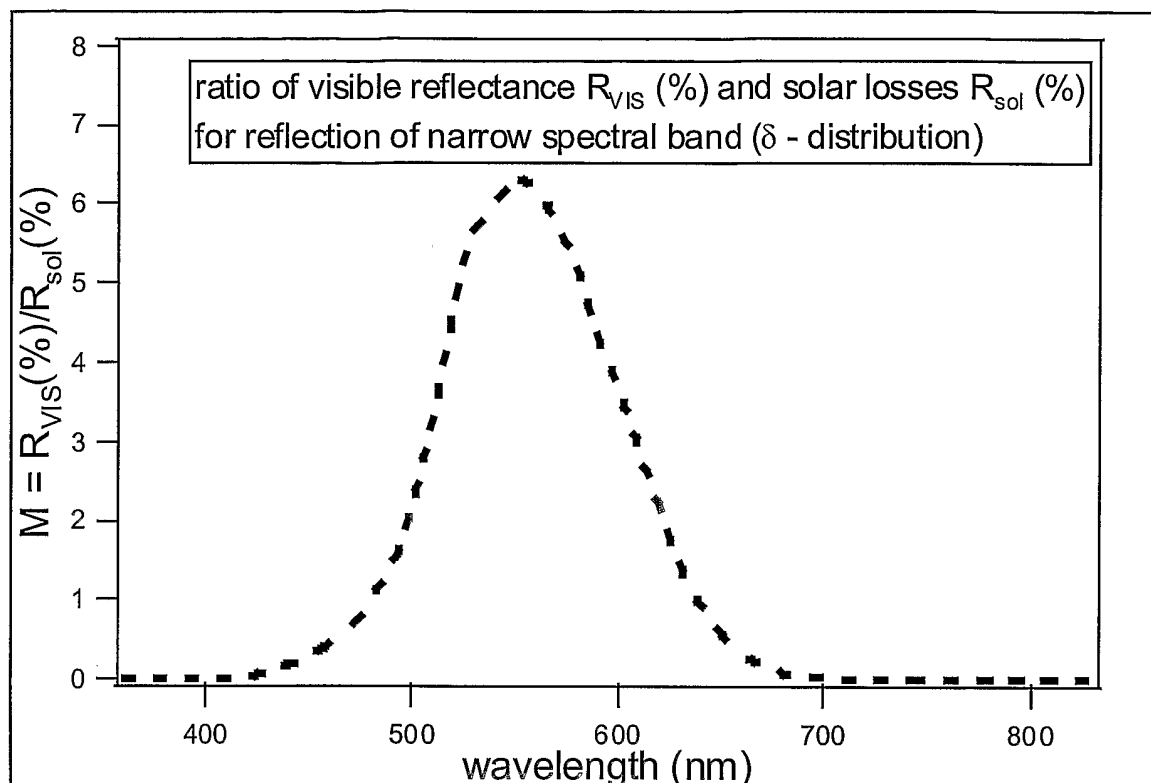




FIG. 2



**FIG. 3**



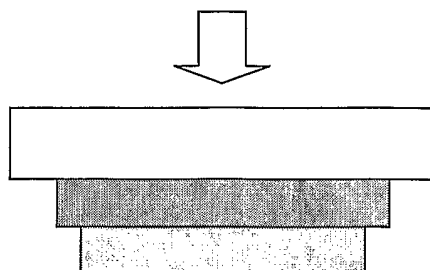
**FIG. 4**air  $n = 1$ glass  $n = 1.52$ TiO<sub>2</sub>  $n = 2.2$ , varying thicknessSiO<sub>2</sub>  $n = 1.46$ , 140 nmair  $n = 1$ 

FIG. 5

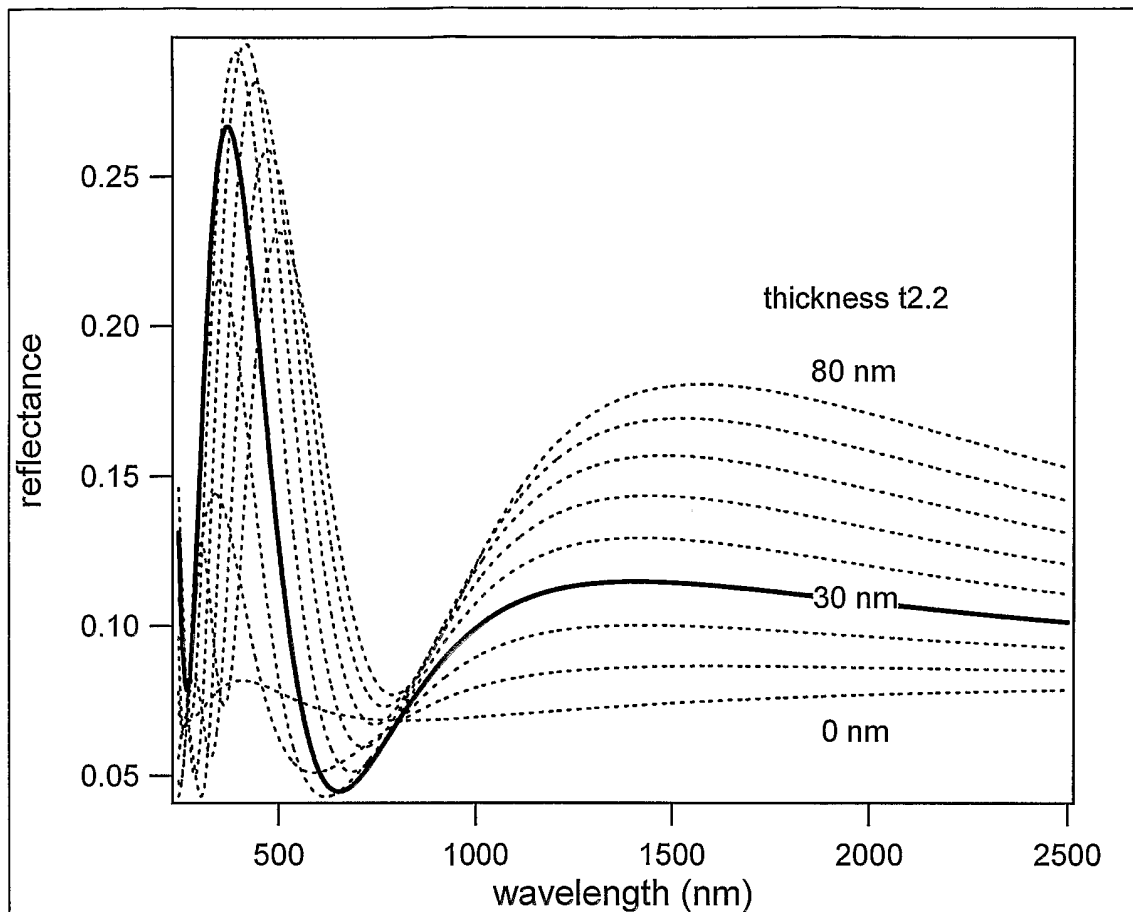
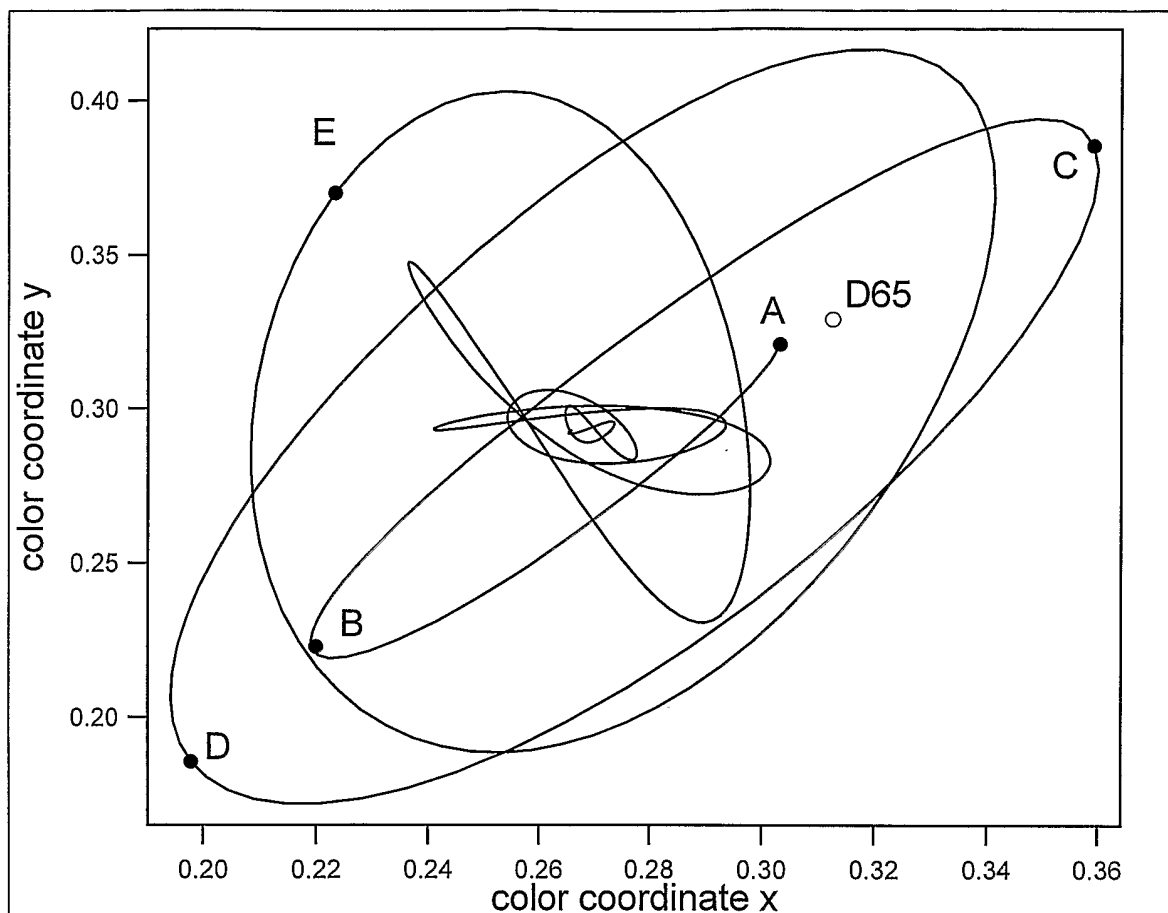


FIG. 6



**FIG. 7**

air  $n = 1$

MgF<sub>2</sub>  $n = 1.38$

TiO<sub>2</sub>  $n = 2.2$

glass  $n = 1.52$

TiO<sub>2</sub>  $n = 2.2$

MgF<sub>2</sub>  $n = 1.38$

air  $n = 1$

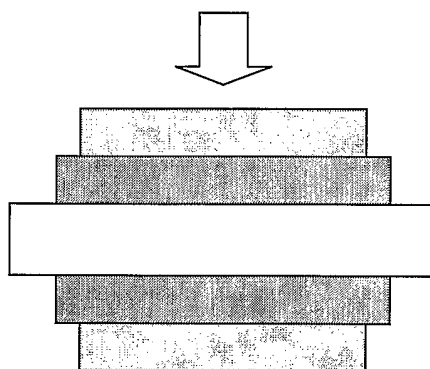


FIG. 8

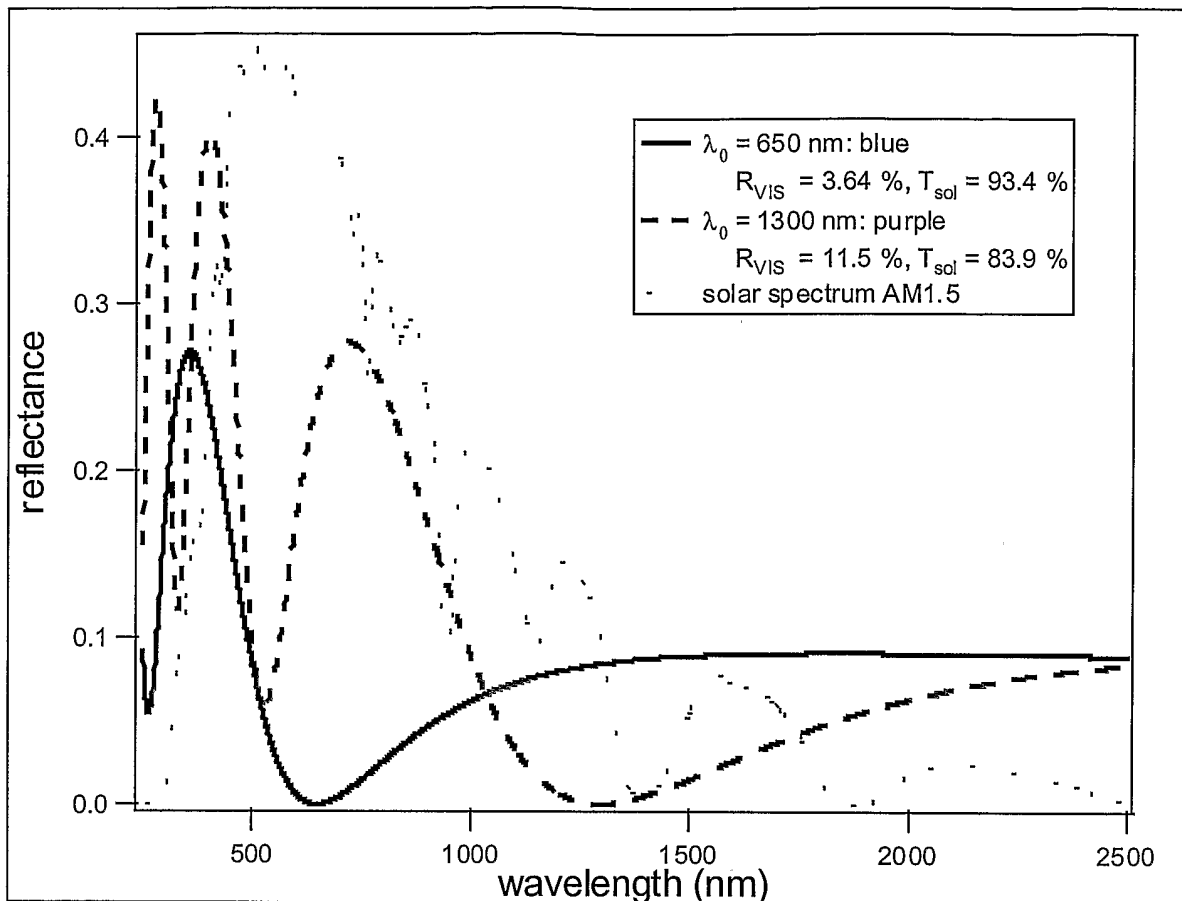
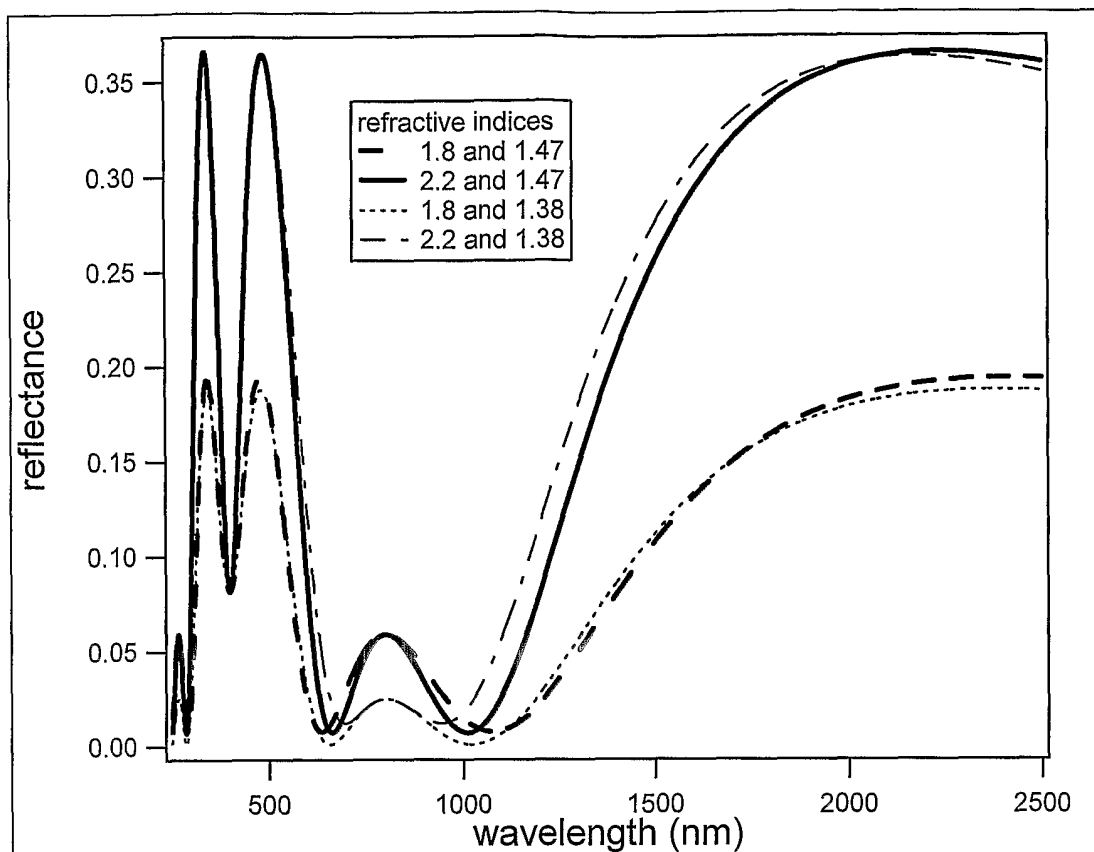


FIG. 9





**FIG. 10**

|                  | n    | thickness (nm) |
|------------------|------|----------------|
| Air              | 1    |                |
| TiO <sub>2</sub> | 2.2  | 0 - 50         |
| SiO <sub>2</sub> | 1.46 | 140            |
| TiO <sub>2</sub> | 2.2  | 30             |
| Glass            | 1.52 |                |
| Air              | 1    |                |

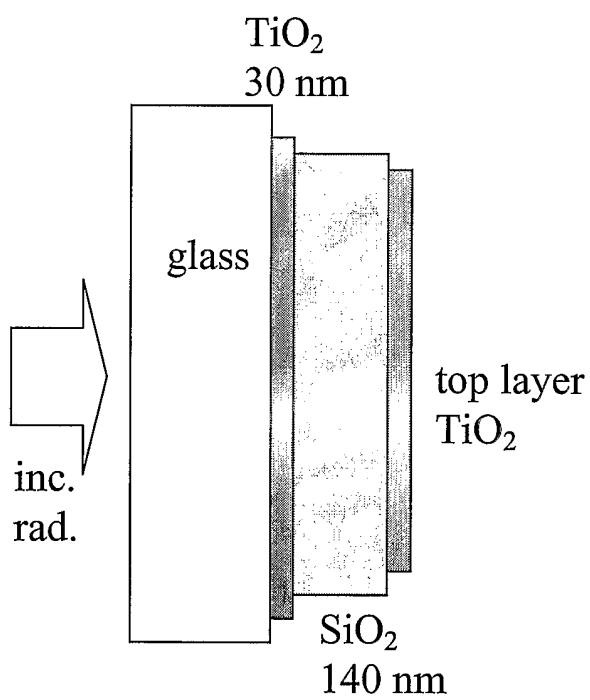


FIG. 11

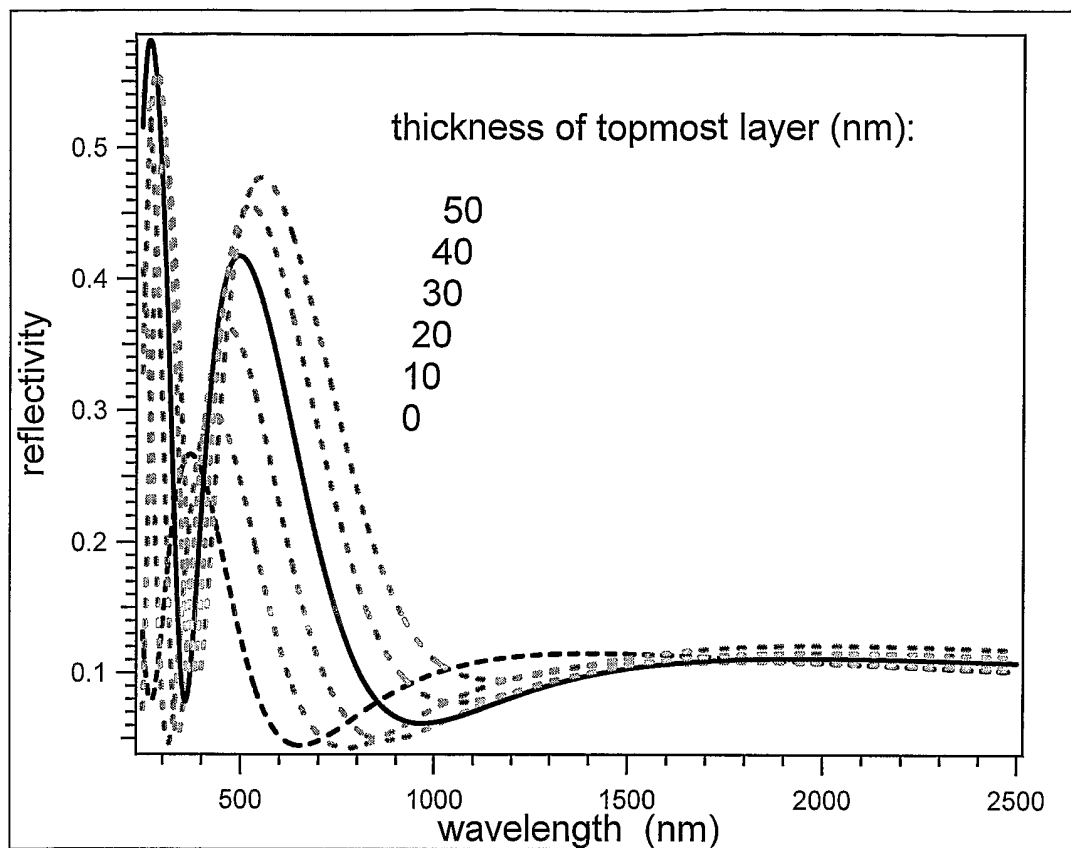
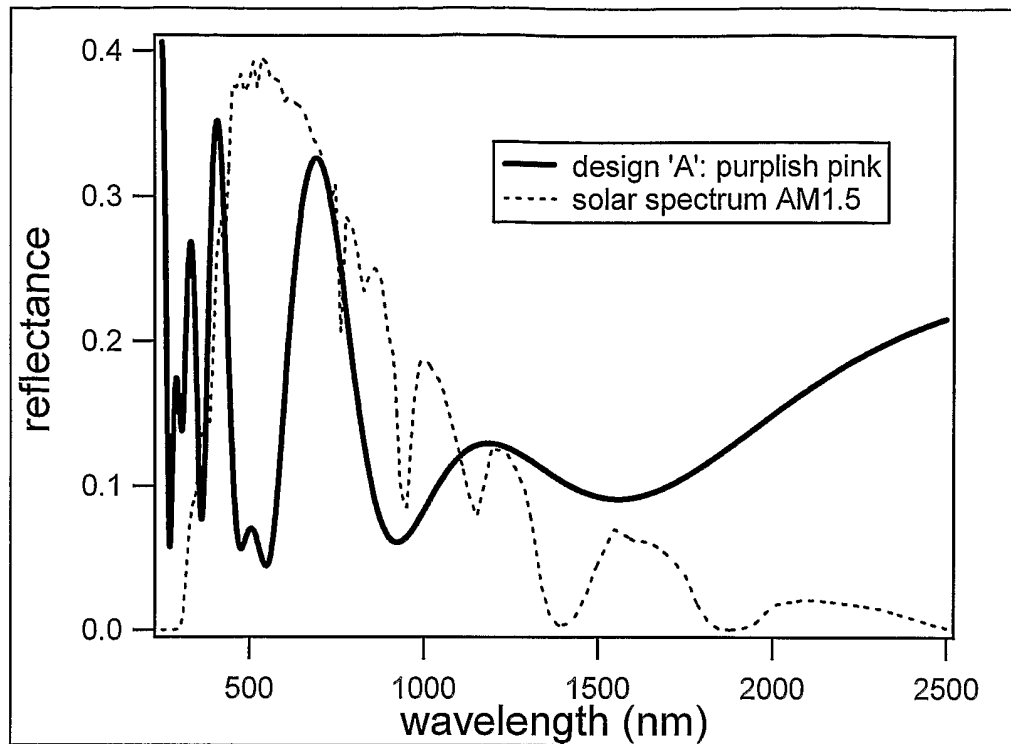


FIG. 12



**FIG. 13**

glass  $n = 1.52$

L:  $n = 1.47$ , 93.5 nm

H:  $n = 1.5$ , 91.7 nm

·  
· 40 layers: (LH)<sup>20</sup>  
·

L:  $n = 1.47$ , 93.5 nm

H:  $n = 1.5$ , 91.7 nm

air  $n = 1$

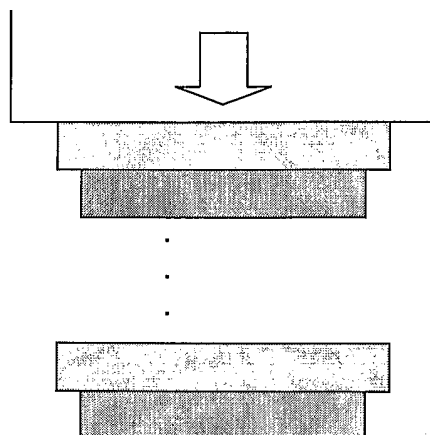
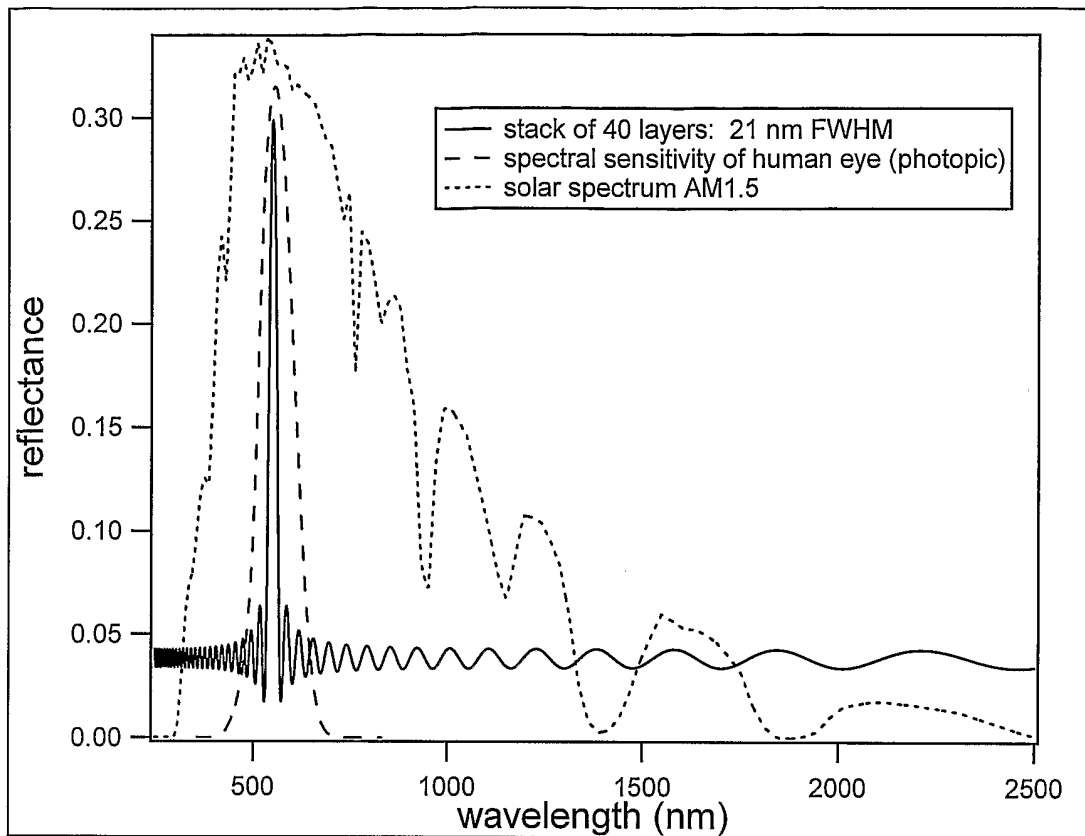
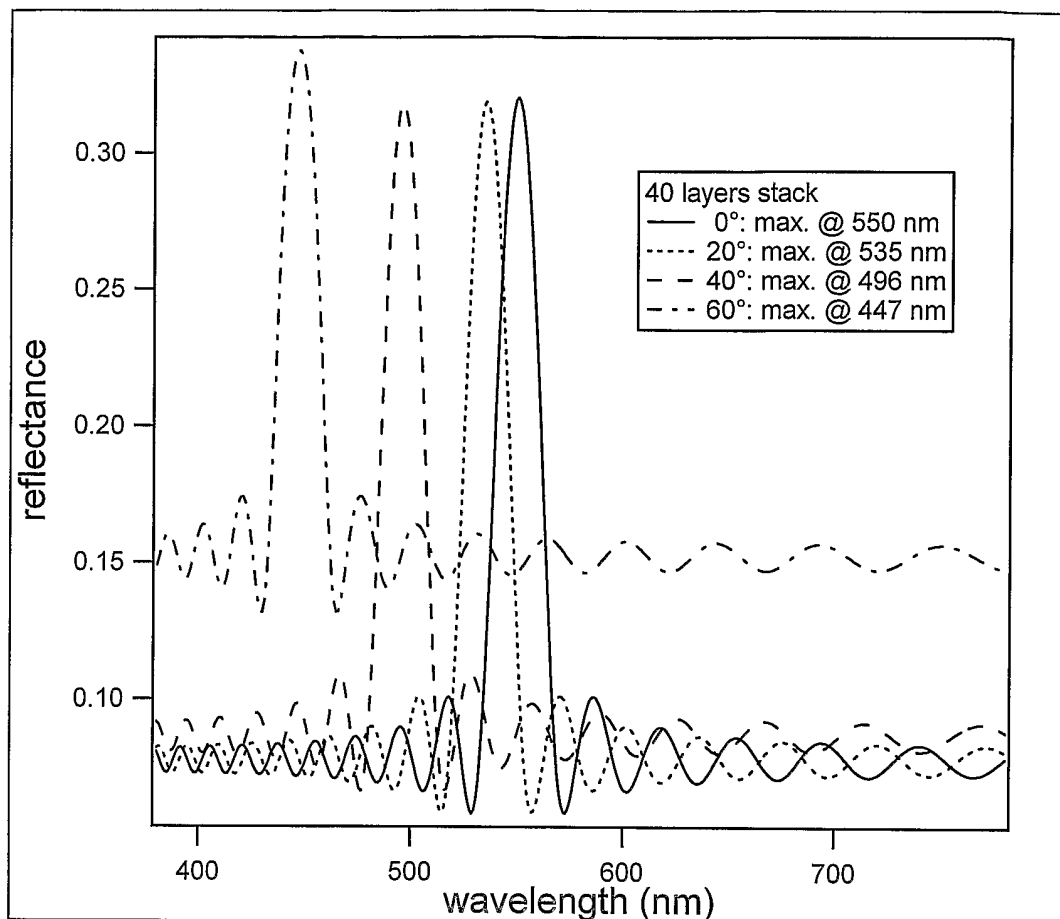


FIG. 14



**FIG. 15**



**FIG. 16**

glass  $n = 1.52$

H:  $n = 1.65$ , 83 nm

L:  $n = 1.47$ , 93 nm

⋮  
 2m + 1 layers: (HL)<sup>m</sup> H

H:  $n = 1.65$ , 83 nm

L:  $n = 1.47$ , 93 nm

H:  $n = 1.65$ , 83 nm

air  $n = 1$

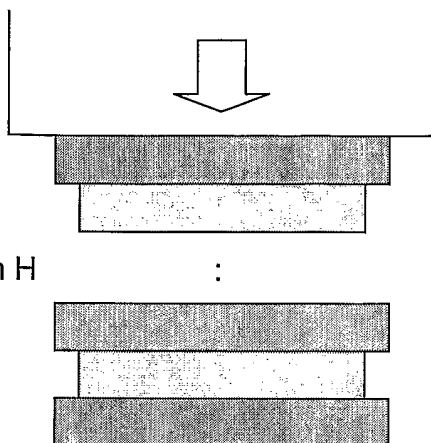


FIG. 17

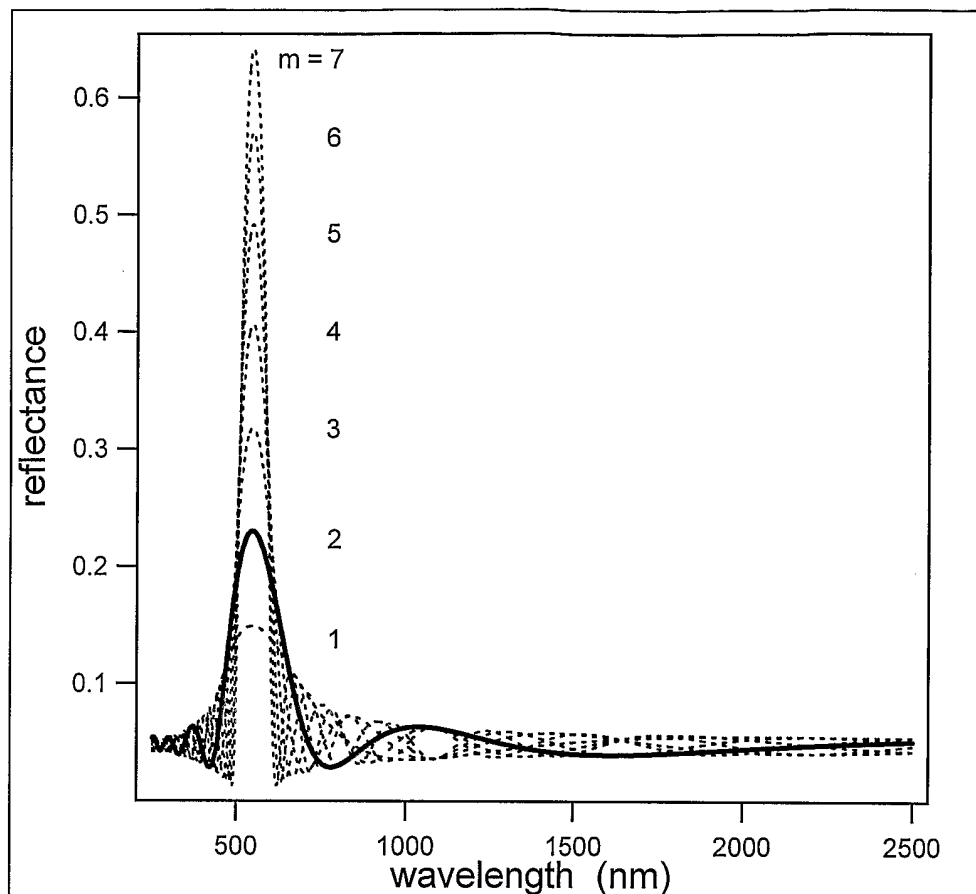
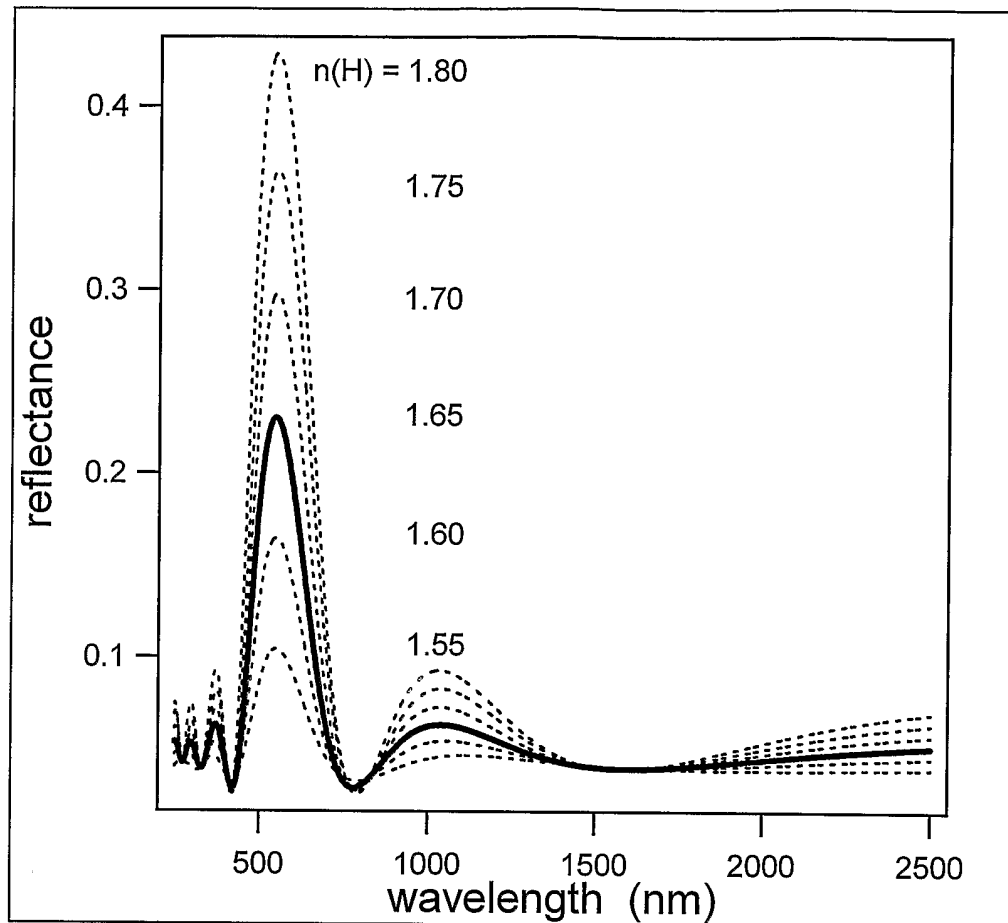




FIG. 18



**FIG. 19**

glass  $n = 1.52$

L:  $n(L), t(L)$

H:  $n(H), t(H)$

air  $n = 1$

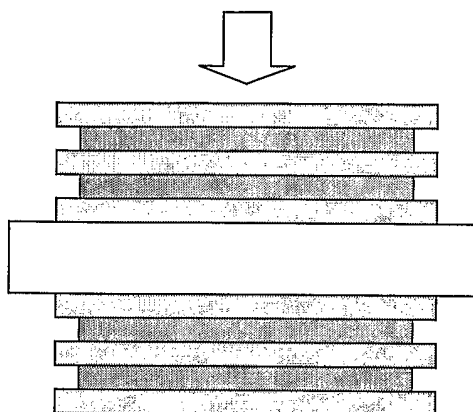
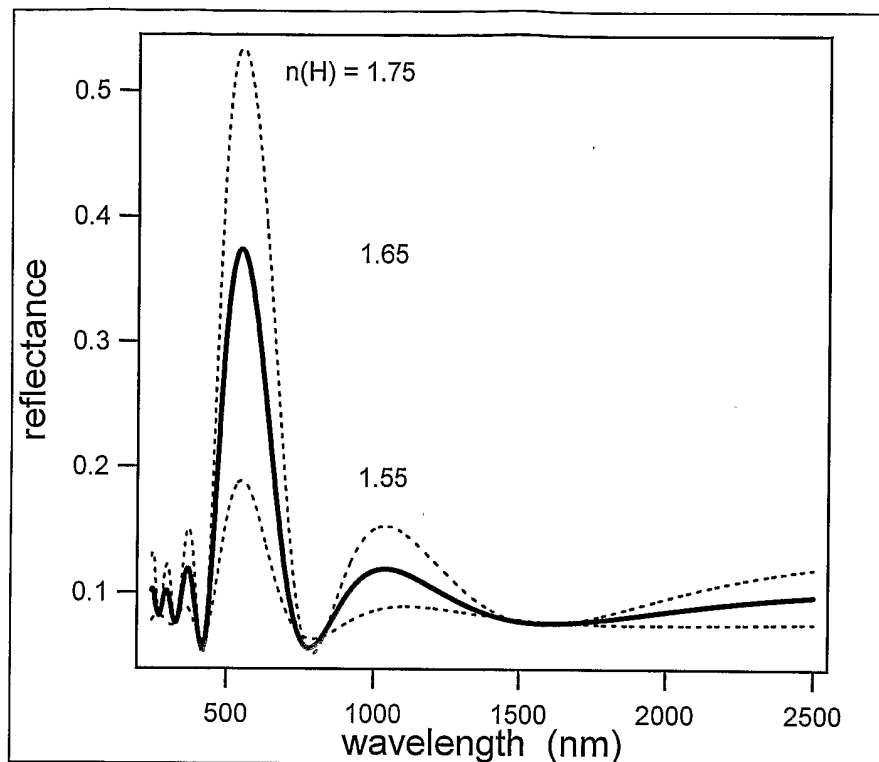


FIG. 20



**FIG. 21**

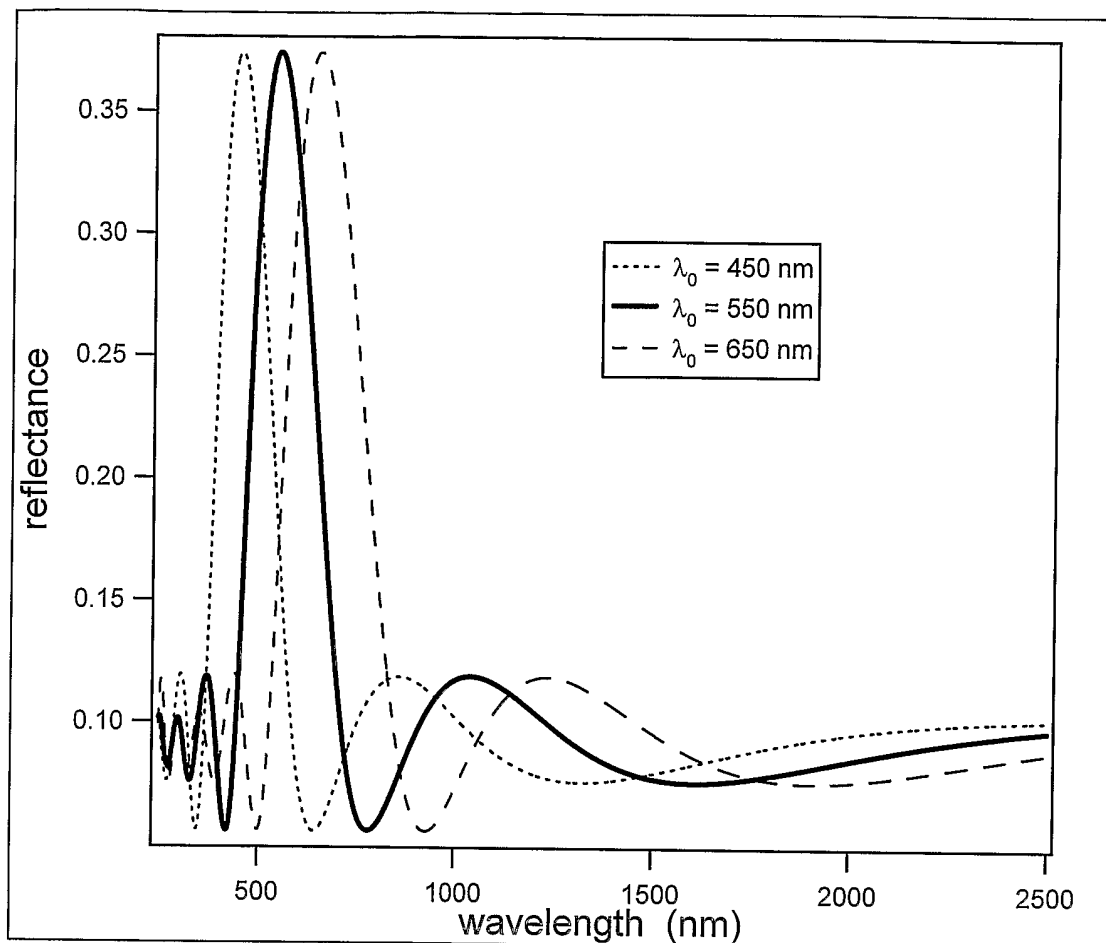


FIG. 22

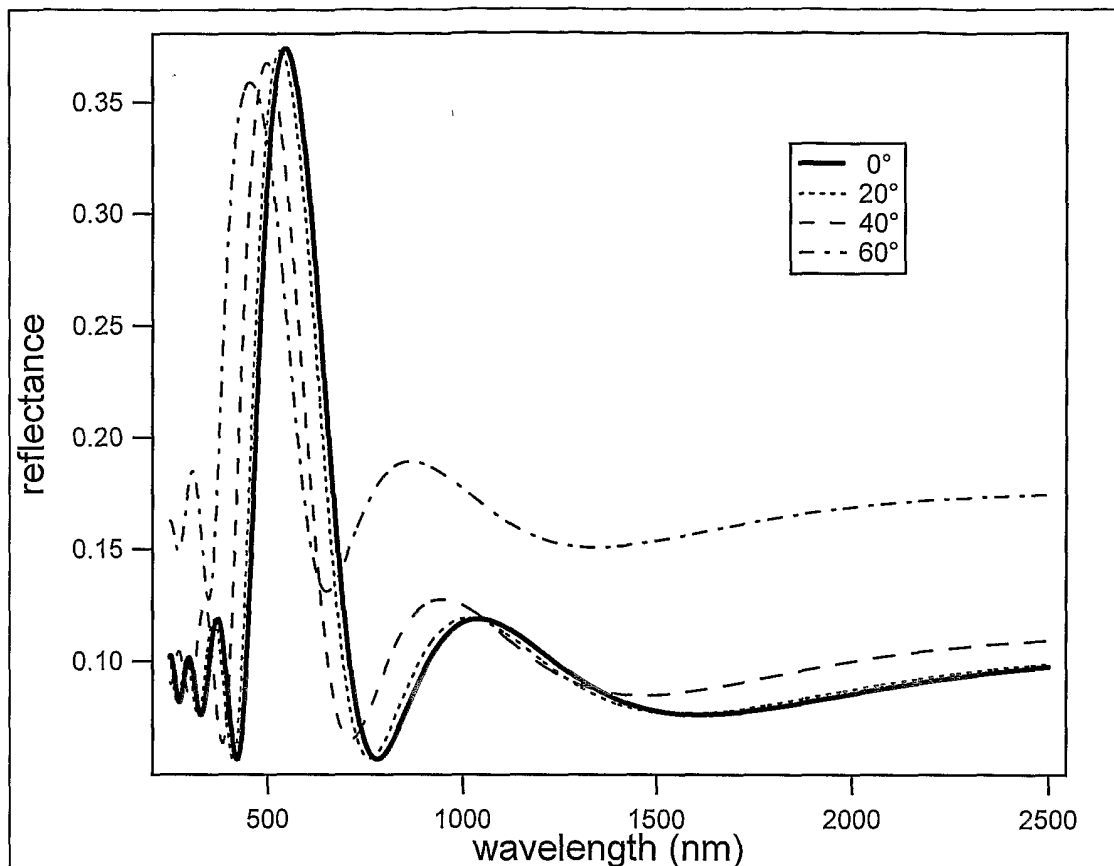


FIG. 23

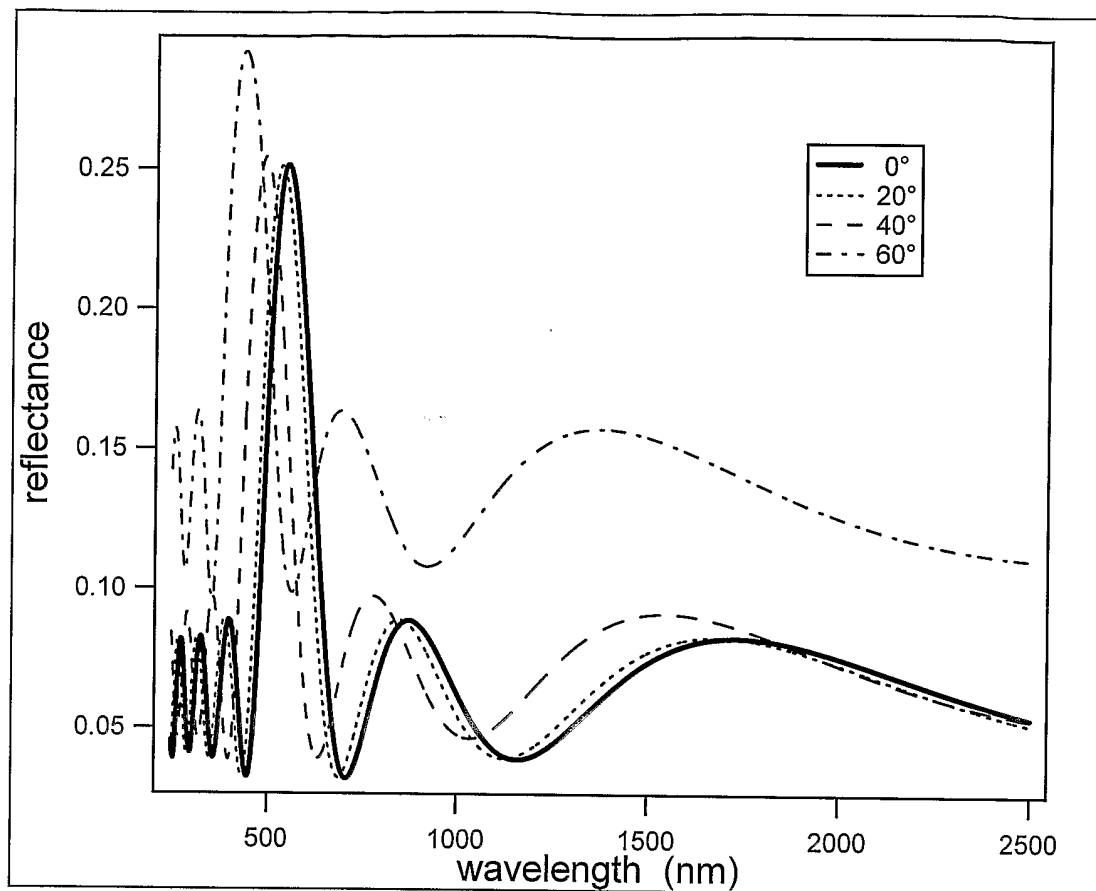
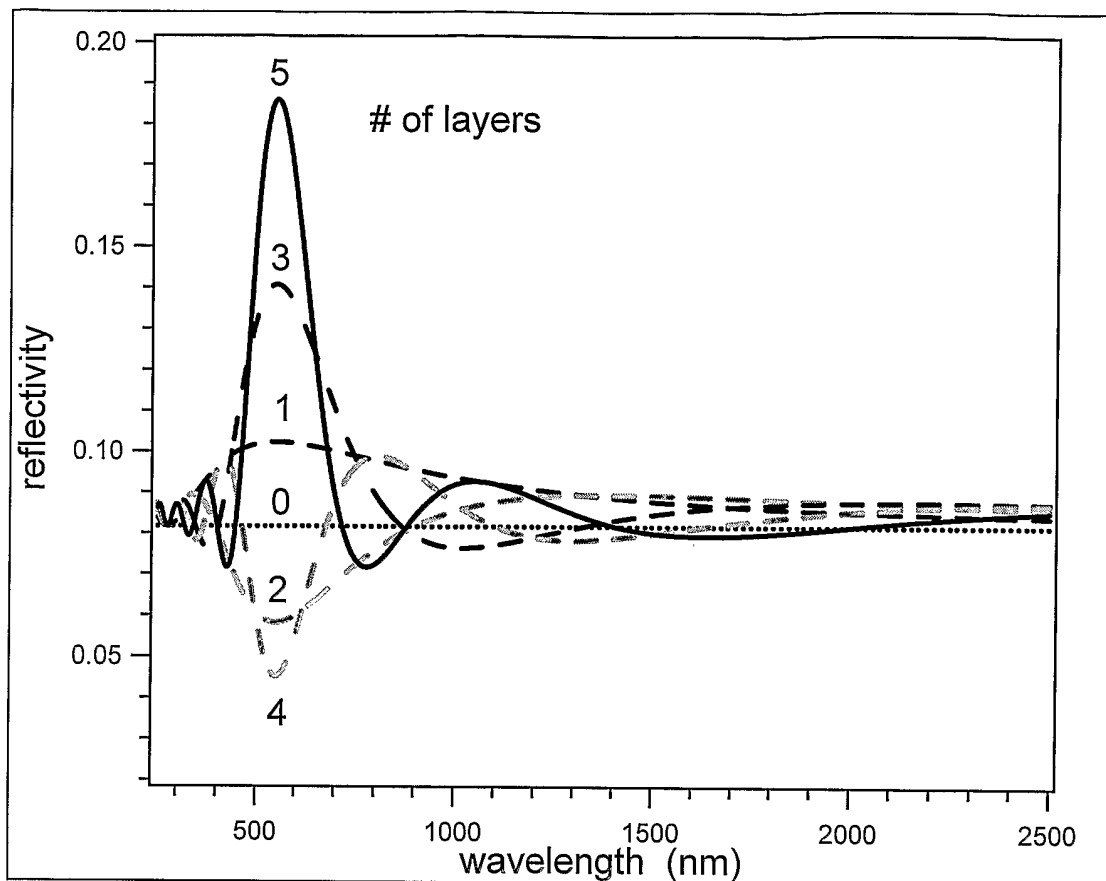


FIG. 24



## INTERNATIONAL SEARCH REPORT

International Application No  
PCT/CH2004/000130A. CLASSIFICATION OF SUBJECT MATTER  
IPC 7 F24J2/50

According to International Patent Classification (IPC) or to both national classification and IPC

## B. FIELDS SEARCHED

Minimum documentation searched (classification system followed by classification symbols)  
IPC 7 F24J G02B C03C

Documentation searched other than minimum documentation to the extent that such documents are included in the fields searched

Electronic data base consulted during the international search (name of data base and, where practical, search terms used)

EPO-Internal, WPI Data, PAJ

## C. DOCUMENTS CONSIDERED TO BE RELEVANT

| Category ° | Citation of document, with indication, where appropriate, of the relevant passages                                      | Relevant to claim No. |
|------------|---|-----------------------|
| X          | WO 02/103453 A (OYA TARO ; SHINGU TADASHI (JP); TEIJIN LTD (JP))<br>27 December 2002 (2002-12-27)<br>abstract; figures  | 1-3                   |
| E          | -& EP 1 398 660 A (TEIJIN LTD)<br>17 March 2004 (2004-03-17)<br>paragraph '0014! - paragraph '0019!;<br>figures         | 1-3                   |
| A          | -----<br>US 4 896 928 A (PERILLOUX BRUCE E ET AL)<br>30 January 1990 (1990-01-30)<br>abstract; figures                  | 1                     |
| A          | -----<br>US 4 546 050 A (AMBERGER CHARLES J ET AL)<br>8 October 1985 (1985-10-08)<br>abstract; figures<br>-----<br>-/-- | 1                     |

 Further documents are listed in the continuation of box C. Patent family members are listed in annex.

° Special categories of cited documents :

- \*A\* document defining the general state of the art which is not considered to be of particular relevance
- \*E\* earlier document but published on or after the international filing date
- \*L\* document which may throw doubts on priority claim(s) or which is cited to establish the publication date of another citation or other special reason (as specified)
- \*O\* document referring to an oral disclosure, use, exhibition or other means
- \*P\* document published prior to the international filing date but later than the priority date claimed

- \*T\* later document published after the international filing date or priority date and not in conflict with the application but cited to understand the principle or theory underlying the invention
- \*X\* document of particular relevance; the claimed invention cannot be considered novel or cannot be considered to involve an inventive step when the document is taken alone
- \*Y\* document of particular relevance; the claimed invention cannot be considered to involve an inventive step when the document is combined with one or more other such documents, such combination being obvious to a person skilled in the art.
- \*&\* document member of the same patent family

Date of the actual completion of the international search

13 July 2004

Date of mailing of the international search report

22/07/2004

Name and mailing address of the ISA

European Patent Office, P.B. 5818 Patentlaan 2  
NL - 2280 HV Rijswijk  
Tel. (+31-70) 340-2040, Tx. 31 651 epo nl,  
Fax: (+31-70) 340-3016

Authorized officer

Van Dooren, M



## INTERNATIONAL SEARCH REPORT

International Application No  
PCT/CH2004/000130

| C.(Continuation) DOCUMENTS CONSIDERED TO BE RELEVANT |   |                       |
|--|---|-----------------------|
| Category °   | Citation of document, with indication, where appropriate, of the relevant passages                        | Relevant to claim No. |
| A  | EP 1 053 980 A (NIPPON SHEET GLASS CO LTD)<br>22 November 2000 (2000-11-22)<br>abstract; figures<br>----- | 1                     |
| A  | EP 0 786 676 A (FLEX PRODUCTS INC)<br>30 July 1997 (1997-07-30)<br>the whole document<br>-----            | 1                     |
| A  | US 4 273 098 A (SILVERSTEIN SETH D)<br>16 June 1981 (1981-06-16)<br>the whole document<br>-----           | 9                     |
| A  | US 4 822 120 A (BACHNER FRANK J ET AL)<br>18 April 1989 (1989-04-18)<br>the whole document<br>-----       | 9                     |

## INTERNATIONAL SEARCH REPORT

Information on patent family members

International Application No  
PCT/CH2004/000130

| Patent document cited in search report |   | Publication date | Patent family member(s) | Publication date |
|--|---|------------------|-------------------------|------------------|
| WO 02103453                            | A | 27-12-2002       | JP 2003075920           | A 12-03-2003     |
|  |   |                  | EP 1398660              | A1 17-03-2004    |
|  |   |                  | WO 02103453             | A1 27-12-2002    |
|  |   |                  | TW 567389               | B 21-12-2003     |
|  |   |                  | US 2004004760           | A1 08-01-2004    |
| EP 1398660                             | A | 17-03-2004       | JP 2003075920           | A 12-03-2003     |
|  |   |                  | EP 1398660              | A1 17-03-2004    |
|  |   |                  | US 2004004760           | A1 08-01-2004    |
|  |   |                  | WO 02103453             | A1 27-12-2002    |
|  |   |                  | TW 567389               | B 21-12-2003     |
| US 4896928                             | A | 30-01-1990       | NONE                    |                  |
| US 4546050                             | A | 08-10-1985       | CA 1279535              | C 29-01-1991     |
|  |   |                  | MX 166886               | B 11-02-1993     |
| EP 1053980                             | A | 22-11-2000       | JP 2001002449           | A 09-01-2001     |
|  |   |                  | EP 1053980              | A1 22-11-2000    |
| EP 0786676                             | A | 30-07-1997       | EP 0786676              | A2 30-07-1997    |
|  |   |                  | AT 172545               | T 15-11-1998     |
|  |   |                  | CA 2048564              | A1 17-02-1992    |
|  |   |                  | DE 69130383             | D1 26-11-1998    |
|  |   |                  | DE 69130383             | T2 11-03-1999    |
|  |   |                  | EP 0472371              | A1 26-02-1992    |
|  |   |                  | HK 1012719              | A1 31-03-2000    |
|  |   |                  | JP 3041094              | B2 15-05-2000    |
|  |   |                  | JP 6118229              | A 28-04-1994     |
|  |   |                  | US 5214530              | A 25-05-1993     |
| US 4273098                             | A | 16-06-1981       | NONE                    |                  |
| US 4822120                             | A | 18-04-1989       | US 4721349              | A 26-01-1988     |
|  |   |                  | JP 51066841             | A 09-06-1976     |
|  |   |                  | JP 60185903             | A 21-09-1985     |
|  |   |                  | US 4337990              | A 06-07-1982     |